Sensors and Actuators A 250 (2016) 250–257

Contents lists available at ScienceDirect

Sensors and Actuators A: Physical

journal homepage: www.elsevier.com/locate/sna

Fabrication and characterization of V_2O_5 nanorods based metal–semiconductor–metal photodetector

N.M. Abd-Alghafour[a,b,*], Naser. M. Ahmed[b], Z. Hassan[c]

[a] Iraqi Ministry of Education, Anbar, Iraq
[b] Nano–Optoelectronics Research and Technology Laboratory School of Physics, University Sains Malaysia, 11800, Malaysia
[c] Institute of Nano Optoelectronics Research and Technology (INOR), Universiti Sains Malaysia, 11800 USM, Penang, Malaysia

ARTICLE INFO

Article history:
Received 15 May 2016
Received in revised form 17 August 2016
Accepted 2 September 2016
Available online 4 September 2016

Keywords:
V_2O_5 NRs
Metal–semiconductor–metal
Visible detector
Responsivity

ABSTRACT

The fabrication and characterization of a metal–semiconductor–metal (MSM) visible photodetector based on V_2O_5 NRs are investigated. V_2O_5 nanorods (NRs) is synthesized on p-type Si(100) by spray pyrolysis method. The MSM photodetector is based on V_2O_5 NRs grown on Si(100) substrate. Structural and optical properties of the V_2O_5 NRs are studied using high resolution X-ray diffraction, field emission-scanning electron microscopy and photoluminescence spectroscopy. The results reveal an orthorhombic structure with preferred orientation along (001) plane of the prepared V_2O_5 NRs. Photoluminescence (PL) spectra show intensive and sharp green light emission at about 535 nm with high intensity. Upon exposure illumination to 540 nm (1.535 mW/cm^2) at an applied voltage of 5 V, the device Exhibit 260.96×10^2 sensitivity; photodetector gain of device is 270, photoresponse peak of 0.948 A/W and photocurrent of 2.7×10^{-4}A. The response and recovery times are determined as 0.787 s and 0.541 s, respectively; upon exposure to 540 nm light at 5 V applied bias. The obtained results indicate that the V_2O_5 NRs is a promising candidate for high performance as a MSM photodetector for commercially photoelectronic applications.

1. Introduction

V_2O_5 is an important transition-metal oxide semiconductor that has gained significant interest in microelectronic and optoelectronic devices in recent times [1]. It is a promising material for the photodetection application due to its direct band gap in the visible-light region (E_g = 2.2 to 2.7 eV) [2] that make it a potential material for use in the optoelectronic devices [3]. Crystalline V_2O_5 exists in unique orthorhombic layered structure, it has the following features: direct optical energy gap, good chemical property, thermal stability, excellent specific energy [4,5]. These properties have made V_2O_5 one of the promising materials for different applications, such as window for solar cells [6], infrared detectors [7], gas sensor [8], catalyst [9] and optoelectronic devices [10]. For light detection, various types of solid-state photodetectors (PDs) such as Schottky diodes type [11], p–n junction type [12], photoconductors [13] and metal–semiconductor–metal (MSM) type [14]. Among these structures, the MSM photodetector has many advantages for useful applications, such as simple fabrication design, inherent high speed, low dark current and compatibility with semiconductor planar technology [15]. MSM-photodetector is promising in military and civil applications. Moreover, MSM photodetector achieve high visible responsivity when high dark current and undesirable continuous photoconductive effects are obtained due to the substoichiometry and low crystallinity of V_2O_5 thin films. To improved device performance, the crystallinity of the V_2O_5 films must be enhanced and oxygen vacancies at the thin film surface reduced during material growth. A wide variety of strategies have been improved to enhance MSM photodetector of V_2O_5. Preparation of V_2O_5 nanostructures, such as nanorods (NRs), characterizes these sustained efforts. The literature survey shows that V_2O_5 nanostructures can be obtained by several different techniques, such as chemical vapor deposition [16], magnetron sputtering [17], sol–gel method [18], pulsed laser deposition [19], electron beam evaporation [20], hydrothermal [21] and spray pyrolysis [22]. Among the various deposition techniques for the preparation of vanadium oxide thin films, spray pyrolysis technique is a relatively simple and inexpensive technique for large-area coatings. It also offers several advantages over conventional deposition techniques for the control of stoichiometry and thin film structure [23]. V_2O_5 nanostructure has been gain notice considerably because they display a range of properties, such as high stability,

* Corresponding author at: Iraqi Ministry of Education, Anbar, Iraq.
E-mail address: na2013bil@gmail.com (N.M. Abd-Alghafour).

http://dx.doi.org/10.1016/j.sna.2016.09.001
0924-4247/

inexpensive preparation and the significantly large energy density [24]. One-dimensional nanostructures such as nanorods play a prominent roles in functional device due to their dimensionality and quantum confinement phenomena [25]. Many researchers in the field have been developed to obtain 1D-V_2O_5 nanostructures. Chen et al. [26] designed an MSM photodetector based on V_2O_5 nanostructure that were obtained using physical vapor deposition method. They achieved responsivity (0.005 A/W) at 0.1 V applied bias voltage with light illumination of 325 nm. Wang et al. [27] fabricated UV photodetector with quite sensible photosensitivity, little change in photo resistance under illuminance ratio 254/365 nm based on high crystallinity quality of V_2O_5 thin films deposited on Si substrate. Suresh et al. [24] investigated the p–n junction properties of V_2O_5 based on p-Si substrate with Ag electrodes. The literature shows that in most of the previous studies, various researchers have used UV light illumination to fabricate UV photodetector based on V_2O_5 nanostructures prepared on Si substrates by different methods. To the best of our knowledge the synthesize of the V_2O_5 NRs on the Si(100) substrate and the fabrication of MSM visible photodetector has not been previously conducted with high responsivity. In the present work, visible light illumination has been used to synthesize a photodetector based on V_2O_5 NRs. The photodetector was fabricated with the aim of manufacturing a visible detector that exhibits high sensitivity to visible light at low-bias voltage, fast response, fast recovery time, uncomplicated low-cost fabrication, and environment-friendly feature. Furthermore, in this work, we have used spray pyrolysis technique to prepare V_2O_5 NRs on the Si(100) substrates which is relatively very simple and inexpensive technique as compared to the conventional deposition techniques. The crystallinity and surface morphology of obtained V_2O_5 NRs were studied during XRD diffraction and field emission-scanning electron microscopy. The electrical and optical properties of the device were also investigated.

2. Experimental details

V_2O_5 thin film were deposited on Si(100) substrates using spray pyrolysis technique. The substrates were cleaned with acetone solution in an ultrasonic bath, rinsed with deionized water, and dried with pure nitrogen gas. VCl_3 powder (purity 99%, purchased from Sigma Aldrich) was mixed with 50 ml deionized water (Millipore, USA). After stirring for 1 h at (27 °C) room temperature, a homogeneous solution (0.05 M) was achieved. In the spray pyrolysis system, compressed air was used as carrier gas with 6 N/cm^2 pressure to spray the precursor solution on to the Si substrates. The deposition spray rate was maintained at 5 ml/min, the distance between spray nozzle and the Si substrate was fixed at 35 cm. The substrate temperature was controlled at 350 °C using a digital temperature controller with an accuracy of ±5.

The structural studies and morphological analysis of the obtained V_2O_5 NRs were characterized using X-ray diffractometer (Model: PANalytical X'Pert Pro) system operating with Cu-Kα radiation λ = 1.54056 Å) at 40 kV and 30 mA and field emission-scanning electron microscopy (Leo Supra 50VP, Carl Zeiss, Germany) equipped with an energy-dispersive X-ray (EDX) system. Optical properties were examined using a Raman spectrometer system (Horiba Jobin Yuon HR 800UV, Edi-son, NJ, USA) with Ar^+ as the excitation source operated at a wavelength of 514.55 nm (20 mW) and a photoluminescence (PL) spectroscopy (Jobin Yvon HR 800 UV, Edison, NJ, USA) with an He–Cd laser (325 nm, 20 mW). The current–voltage (*I–V*) measurements were achieved using a computer-controlled integrated source meter (Keithley 2400) at room temperature.

3. Results and discussion

3.1. Structural characterization of V_2O_5 NRs

The XRD diffraction patterns of the V_2O_5 NRs synthesized onto Si(100) substrate by spray pyrolysis method are shown in Fig. 1. The figure shows the formation of diffraction peaks corresponding to V_2O_5 along different planes. A predominant peak was observed in the XRD diffraction pattern at 20.2° which related with the preferred orientation along (001) plane. Furthermore, eight reflection peaks were observed at 2θ values of 15.3°, 21.7°, 26.2°, 31.1°, 32.3°, 34.3°, 41.3° and 44.4° correspond to (200), (101), (110), (301), (011), (310), (002) and (501) reflections of the orthorhombic V_2O_5 material. All XRD peaks matched the orthorhombic phase of V_2O_5 (JCPDS card No. 00-041-1426), except for the low intensity peaks that were associated to the Si substrate. Additionally, the XRD patterns of the V_2O_5 NRs are high intensity and sharp due to the annealing temperature at 500 °C for 1 h, which improved the crystalline quality of the V_2O_5 NRs [24]. The XRD peaks show the formation of high crystallinity orthorhombic phase V_2O_5 which is similar to the results reported by Pavasupree et al. [29], Jinxing Wang et al. [21], Yifu Zhang [30]. These results reveal that the high crystallinity of the V_2O_5 product, which observes no peaks of any other impurities.

The crystallise size along the preferred orientation of V_2O_5 peak was calculated by using the following equation [31];

$$D = \frac{k\lambda}{\beta \cos\theta} \quad (1)$$

where D is the crystallite size, λ is the wavelength of the incident radiation (1.5406 Å), β is the full width half maximum (FWHM) and θ is the Bragg's angle of diffraction. The crystallite size was found to be 29.4 nm. In order to calculate strain along (001) diffraction plane of V_2O_5, the following relation was used;

$$\varepsilon_{zz} = \frac{c - c_0}{c_0} \times 100 \quad (2)$$

where c and c_0 (4.372 Å) are the lattice constant of the V_2O_5 NRs estimated from the XRD data and the standard lattice constant for V_2O_5 material (JCPDS card No. 00-041-1426). The strain of V_2O_5 NRs along (001) plane was found to be 0.45%. The positive value of strain shows the presence of tensile stress inside the V_2O_5.

Fig. 2 displays the FESEM images of the prepared V_2O_5 NRs with two different magnifications. The FESEM images show high-density V_2O_5 NRs and uniform growth that was nearly vertical to the Si substrate. The nanorods have average diameters of 60–80 nm

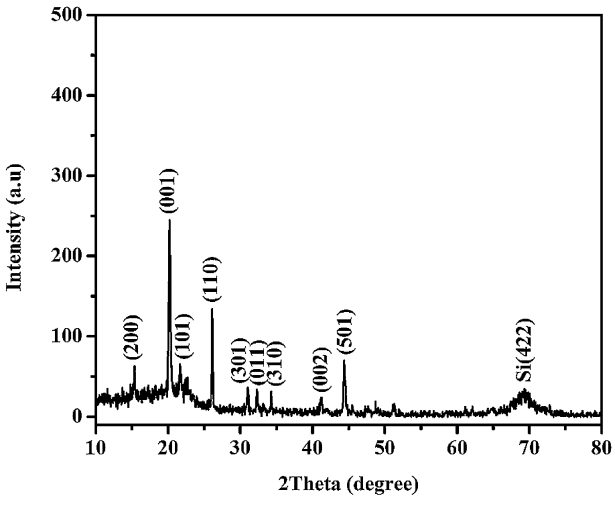

Fig. 1. XRD patterns of the V_2O_5 NRs grown on silicon (100) substrate.

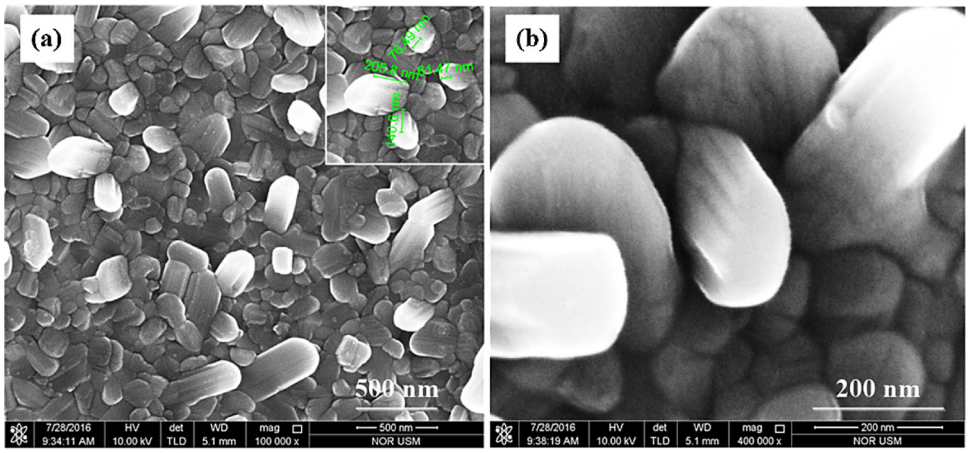

Fig. 2. FESEM images of the V_2O_5 NRs grown on silicon (100) substrate.

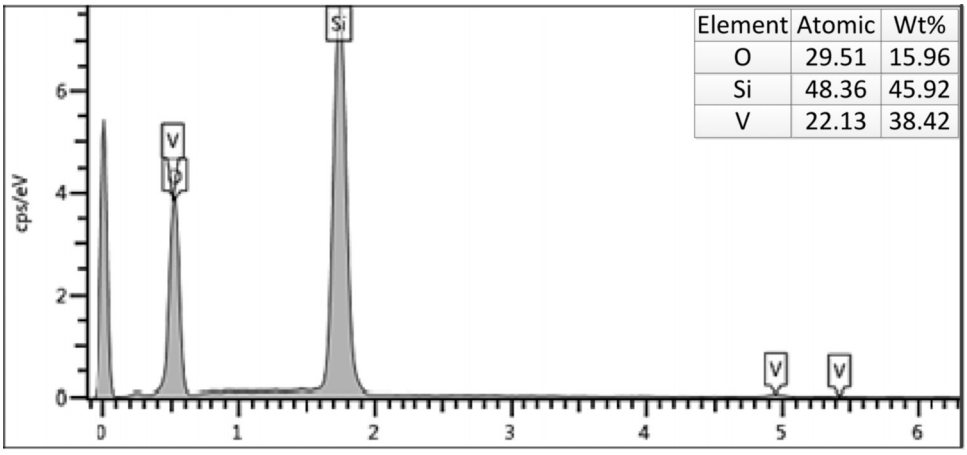

Fig. 3. EDX spectra of the V_2O_5 NRs grown on silicon (100) substrate.

and the length of 200 nm. The V_2O_5 NRs sample has increased number of nucleation locations when the substrate was completely covered with dense nanorods. The nucleation locations functioned as a base for particle congregation. Moreover, the basic groundwork of NRs is formed through the coalescence of congregated particles. Subsequently, the structure grows to specified dimensions on the substrate through particle accumulation [32]. The proportion of vanadium–oxygen is exhibited in Fig. 3. The energy dispersive X-ray (EDX) spectra showed that this prepared samples included 38.42 wt% and 15.96 wt% of V and O, respectively. These values are in consistent with the optimal stoichiometry for the prepared V_2O_5 sample. No elements no other peaks associated to impurities or contamination are detected which assert the purity of V_2O_5 NRs obtained in the current study. Fig. 4 displays the Raman peaks of the V_2O_5 NRs were measured in the wave number range of 100–100 cm^{-1}. The peaks of the prepared V_2O_5 NRs were symmetric with the Raman modes for a V_2O_5 orthorhombic phase [33]. The dominant peak at 143 cm^{-1} was associated to vibrations of the V—O—V chains, and its existence displays the layered orthorhombic structure of the V_2O_5 NRs phase. The peak at 995 cm^{-1} corresponds to the terminal oxygen (V^{+5}=O) stretching mode, which is associated to the crystallinity quality and stoichiometry of the thin films [34]. In the case of the Raman peaks at 523 and 696 cm^{-1} are attributed to V_3O phonon band and V—O—V modes, intensities of both these modes were found to be quite small. The results obtained indicate that significantly improves its structural and optical properties.

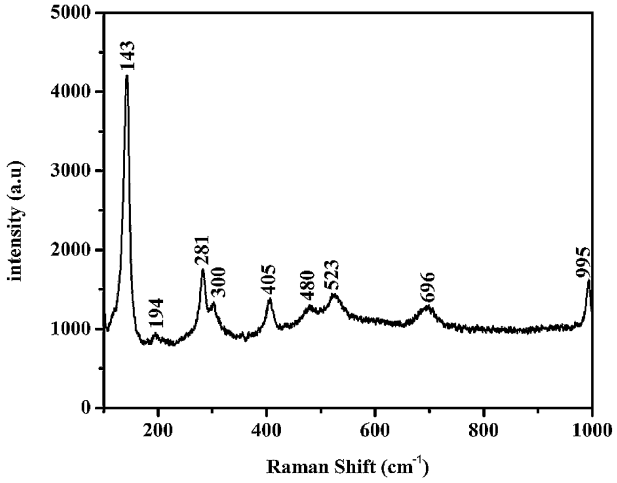

Fig. 4. Raman spectra of the V_2O_5 NRs grown on silicon (100) substrate.

3.2. Optical properties

PL spectra of V_2O_5 NRs prepared using spray pyrolysis method on Si(100) substrate is revealed in Fig. 5. Photoluminescence characteristics of the V_2O_5 thin films are significant because it provides valuable information on the superiority and pureness of the materials. One of the impressive features of semiconductors is their ability

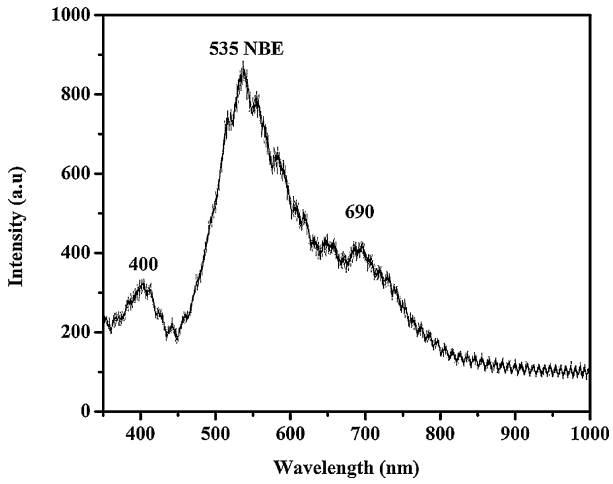

Fig. 5. Photoluminescence spectra at room temperature of the V_2O_5 NRs grown on silicon (100) substrate.

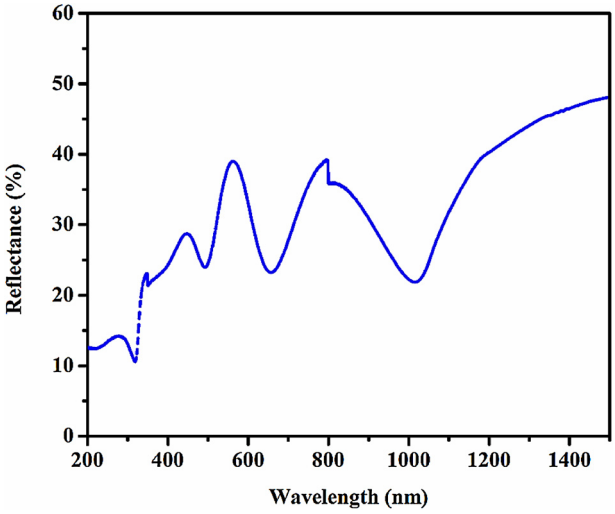

Fig. 6. UV–visible reflectance spectra of the V_2O_5 NRs films grown on silicon (100) substrate.

to emit light. The emission spectra show one high green emission around 535 nm (E_g = 2.3 eV). This peak could be associated to the electron transition between the valence and conduction bands. The optical band gap value was in agreement with previous literature [35,36], that reported values for thin films change between 1.95 and 2.4 eV depending on the crystallinity quality and stoichiometry of the prepared samples and deposition method. As shown in Fig. 5, V_2O_5 NRs displayed a strong green emission is associated to the NBE emission which is due to the recombination of free excitations [24]. However, a broad emission peaks emissions observed at ~690 nm which are attributed to deep level emission (DLE) caused by structural defects, it is agreement with previous measurements [37] and [23].

The defects in thin films could be due to oxygen vacancies which are formed in the O layer between two O—V layers. Empty conduction bands (V-3d) of vanadium atoms adjacent vacancies are able to centralize excess electrons. This is leads to the formation of the emission observed peaked at 690 nm. Strong visible peak compared to weak band intensity in the UV region indicate that V_2O_5 NRs reveal an excellent optical quality structure without impurities and native defects. The PL intensity proportion between (Visible–UV) regions is the significant indicator of good crystallinity and the main identifying characteristic of excellent optical properties. The high PL peak intensity for V_2O_5 NRs is due to the improvement of optical properties of V_2O_5 nanostructures. The high optical properties of the prepared V_2O_5 NRs display that such a structure has high performance for optoelectronic applications.

Fig. 6 shows the UV–visible reflectance spectra of V_2O_5 NRs prepared on Si(100) substrate. These spectra were used to evaluate the optical band gap of thin film at room temperature. The optical measurements were carried out in the range of 200–1500 nm, using Carry 5000 series UV–vis system. The figure shows interference fringes as a wavelength is changed. From the literature, it is well known that, the wavelength at which these interference fringes disappear is called cut-off wavelength and it is the wavelength from which band gap of the film can be determined [38]. From the figure the cut-off wavelength was calculated to be 490 nm. The band gap of V_2O_5 thin film was determined from the following relation;

$$E = hc/\lambda \quad (3)$$

Here E is the energy band gap of V_2O_5 thin film, h is the Planks constant and λ is the wavelength, By putting the value of the cut-off wavelength in this equation, the band gap of V_2O_5 thin film was came out to be 2.45 eV. This result presents the closest value to the PL measurements.

3.3. Device fabrications

The schematic illustration of the fabricated MSM photodetector is revealed in Fig. 7. The MSM-structured device was fabricated by depositing an Ag grid (150 nm thickness) on the V_2O_5 thin film by using vacuum thermal evaporation (Edward Auto 306) at a standard pressure of 3×10^{-5} mbar. The fabricated device contains two interdigitated electrodes with four fingers on each electrode. The dimensions of each finger were 3.4 mm × 0.35 mm × 0.4 mm in

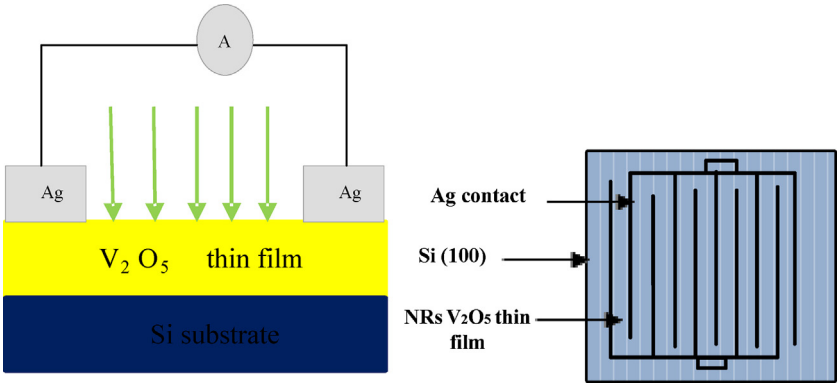

Fig. 7. Schematic diagram of the metal shadow used for the fabrication of MSM photodetector.

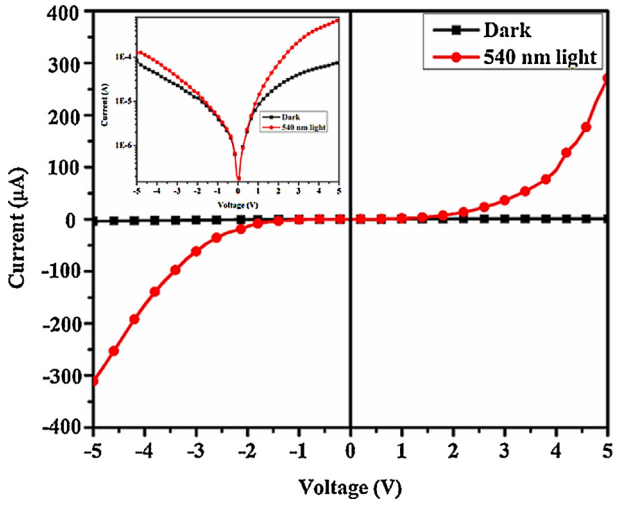

Fig. 8. Current–voltage characteristics of the (Ag/V_2O_5NRs/Ag) MSM photodetector under dark and UV illumination (540 nm, 1.535 mW/cm^2).

length, width, and spacing of metal mask, respectively. The effective area of the device was 0.1634 cm^2.

3.4. Current–voltage (I–V) characteristics

The revealing characteristics of the sample were measured by taking its current–voltage response that is shown in Fig. 8. Current–voltage characteristics have also been plotted on the logarithmic scales that are shown inside Fig. 8. The figure shows that the current in V_2O_5 NRs increases when the sample is illuminated by 540 nm green light, and the incident optical power was 1.535 mW/cm^2 at the distance of 3 cm from a visible lamp to device. The dark current in present work has been found of the order of 3.74×10^{-6}A at −5 V and 5 V bias voltages whereas the photocurrent increases by an order of 2.7×10^{-4}A. This indicates that the MSM photodetector based on V_2O_5 NRs shows good photo-detection characteristics under 540 nm visible light. By comparing the dark current achieved in this work with the previous photodetectors shows that in the present work low dark current has been achieved as compared to the previous studies [39]. The low dark current in the sample is assigned to the formation of V_2O_5 NRs with good crystalline quality and a homogeneous contact at the metal-film interface. Fig. 8 shows that the Schottky contacts have been generated in both directions. The formation of Schottky contact at the metal film interface shows that the V_2O_5 NRs work function is lower that of the Ag that causes electron transfer from the semiconducting film to the metal this the semiconductor is depleted near the junction and hence the Schottky contact is created at the metal-film interface. According to the MSM model, the carrier concentration and conductivity of the V_2O_5 NRs are 1.69×10^{14} cm^{-3} and 0.829 S/cm, respectively. The value of conductivity in this current work is higher than that has been reported by several researchers. Butt et al. [40] was calculated Carrier concentrations, $N_d = 1.48 \times 10^{18}$ and conductivity = 36.1 S/m using the metal–semiconductor–metal (MSM) model. Raman et al. [41] was recorded conductivity = 9.14×10^{-5} S/cm at high temperature. It was found that conductivity increases with increase in annealing temperature. Benmoussa et al. [42] indicated the temperature dependence of the conductivity measurements for V_2O_5 grown by R.F. sputtering method. The results reveals that the conductivity obtained for polycrystalline V_2O_5 thin films is quite low (8.7×10^{-7} S/cm). The *I* transport along the Schottky type photodetectors are qualified by thermionic emission theory by using Eq. (4) [43]:

$$I = I_0 \exp\left(\frac{qV}{nkT}\right)\left[1 - \exp\frac{-qV}{kT}\right] \quad (4)$$

where *q* is the electron charge, *V* is the applied bias voltage, *n* is the ideality factor, *k* is the Boltzmann constant, *T* is the absolute temperature and I_0 is the reverse saturation current, which is calculated by equation:

$$I_0 = AA^{**}T^2 exp\left[\frac{-q_B}{kT}\right] \quad (5)$$

where A^{**} is the effective Richardson constant, *A* is the contact area (in present work $A = 0.326$ cm^2) and Φ_B the effective Schottky barrier height.

Φ_B and *n* were determined from current–voltage using thermionic field emission analysis based on Eqs. (4). Average Φ_B and *n* for the device are determined as 0.919 eV and 7.16, respectively, using $A^* = 50.3$ A/cm^2 K^2.

The sensitivity of the fabricated photodetector was also investigated by measuring the current-time response at different voltages. The current-time graphs of V_2O_5 NRs are shown in Fig. 11. The figure shows an excellent stability and repeatability in the current-time pulses. This is an indication that under the illumination of 540 nm green light, the rises to its peak value and once the light is switched off, the current quickly falls down. By increasing the voltage the magnitude of current also increases that can be clearly seen from the current-time pulse graphs. In order to calculate the sensitivity for these graphs, the following formula was used the following relation [44];

$$(S\%) = \frac{I_{ph} - I_d}{I_d} \times 100 \quad (6)$$

The maximum value of the sensitivity has been found to be 260.96×10^2 at 5 V bias voltages, which exhibits that the device could be useful as optical applications. Photo-generated charges are produced from the applied electric field, when the photodetector was illuminated with the light green. Subsequently, the photocurrent that was added to the bias current effectively increases device conductivity. The sensitivity was approximately seven orders of magnitude larger than that value for the V_2O_5 NWs, which is obtained by Chen et al. [26]. In addition, the current values of response time and recovery time are smaller than those reported by Pawar et al. [45] ($\tau_r = 65$ s, $\tau_d = 75$ s, bias voltage = 5 V for a photodetector based on V_2O_5 nanosheets). For the results value, the responsivity was about one order of magnitude larger than that obtained by Zhai et al. [1] for V_2O_5 NWs on Si substrate. In order to calculate the responsivity of the V_2O_5 thin film over different wavelength range, lights of various wavelengths was illuminated on the sample, and the according to current was calculated. The responsivity of the photodetector was calculated by using the following relation;

$$R = \frac{I_{ph}(A)}{P_{in}(A)} = \frac{I_{ph}(A)}{E\left(W/cm^2\right)A\left(cm^2\right)} \quad (7)$$

where *E* is the radiation of the green light, which is measured by a typical visible power meter (Newport Power meter, Model 2936-CUSA), I_{ph} is the current density and P_{in} is the power density. The photoresponse of the fabricated photodetector was examined under illumination in the ranging of 450 nm to 550 nm at 5 V applied voltages, as revealed in Fig. 9. The figure shows maximum responsivity at 520 nm wavelength and the responsivity starts to decrease below 520 nm and above 530 nm. The cut off wavelength in our case has been found to be 530 nm, which is quite near to the band gap of the V_2O_5 NRs. It means that when a light having wavelength having energy slight higher than the optical band gap of the

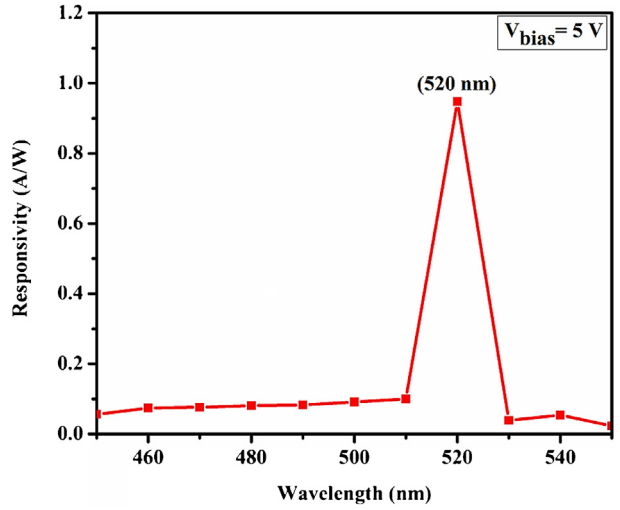

Fig. 9. Room temperature responsivity spectra of the (Ag/V_2O_5NRs/Ag) MSM photodetector.

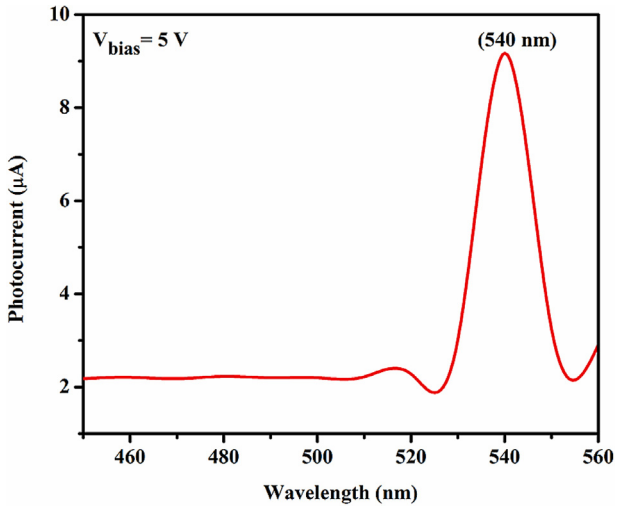

Fig. 10. The (Ag/V_2O_5NRs/Ag) MSM-structured visible-PD photoconductivity versus light wavelength.

thin films is occident to the photodetector, it creates a large number of electron-hole pairs that move under the action of applied potential and thus the photocurrent is produced that shows its maximum value as compared to the other wavelengths where the responsivity starts to fall down. The responsivity starts to fall down at much higher energies that then the band gap energy of the V_2O_5. This is basically due to a decrease in the penetration depth of the incoming light in the film. Thus the photo generated carriers recombine on the top surface without going inside the film thus the current produced is quite low and responsivity shows a decreasing trend. The value of responsivity in our case has been found to be 0.948 A/W, which is higher than previously reports values [46].

Fig. 10 displays that the photocurrent increased at 525 nm wavelength, and decreased at the visible region with 555 nm wavelength. After the wavelength declined, absorption coefficient increased and the permeation depth of visible illumination was reduced. This procedure increased the charge carrier pair concentration of the neighbouring V_2O_5 NRs. Thus, the lifespan of the generated charge carrier's pair was reduced, causing a subsequent decrease in the responsivity. Under radiation of 540 nm wavelength, the high peak was 0.948 A/W. This peak demonstrated that V_2O_5 NRs supplied large density with rougher surface areas,

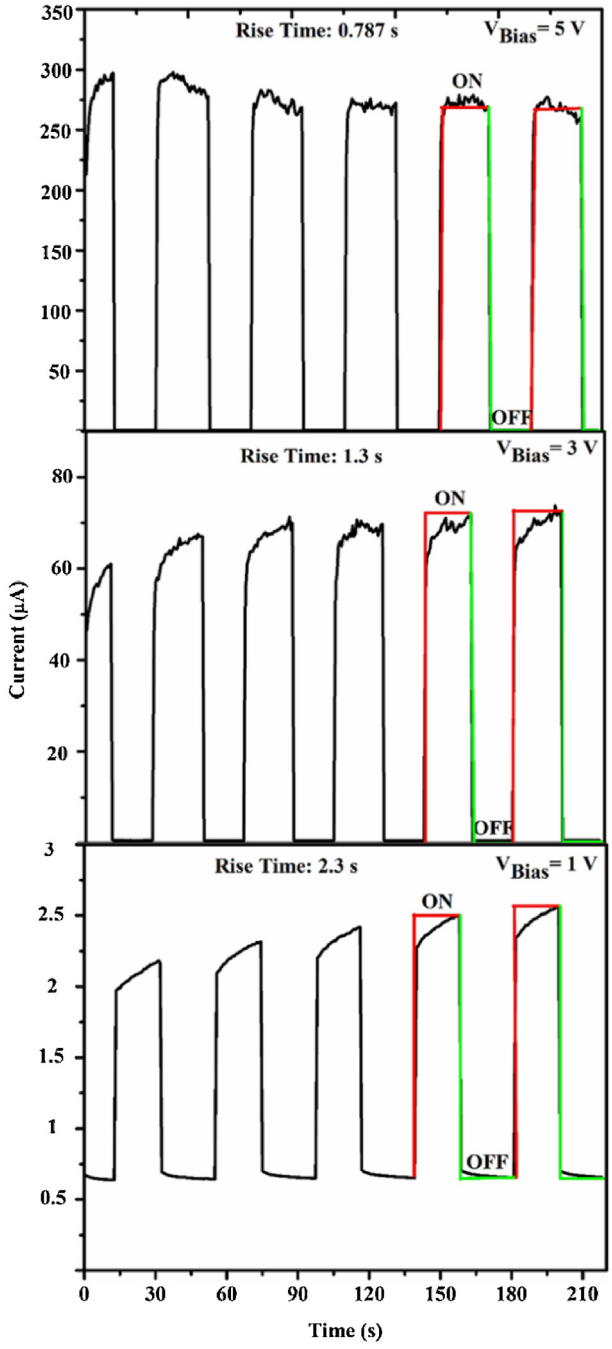

Fig. 11. The repeatability property (ON/OFF) of the V_2O_5 NRs/p-Si(100) MSM photodetector under pulsed visible light (540 nm) at different bias voltages.

and excellent MSM photodetector was formed in the V_2O_5 NRs. The quantum efficiency of a MSM photodetector is well-defined as the number of charge carriers collected to produce the photocurrent created for every number of incident optical power, as in the following equation [47]:

$$\eta\% = \frac{I_{ph}}{q}\frac{h\nu}{p_{in}} \tag{8}$$

This relation can be estimated by determining the photoresponse (R) via:

$$\eta\% = R\frac{hc}{gq\lambda} = \frac{1.24R}{g\lambda\,(\mu m)} \tag{9}$$

Table 1
The comparison between the literature and the current study of the responsivity, the sensitivity, the response and recovery time for the (Ag/V_2O_5NRs/Ag) MSM-structured visible-PD.

Bias voltage (v)	λ (nm)	Responsivity (A/W)	Response time (s)	Recovery time (s)	Sensitivity (%)	Reference
1	540	0.948	0.914	0.573	26.964×10^3	Our work
5	400	0.062	65	75	–	nanosheets [45]
0.1	325	0.005	–	–	300	nanowires [26]
1	450	0.446	–	–	21.6	nanowires [1]
4	450	–	237.1×10^{-6}	93.4×10^{-6}	75	nanobelts [46]

where q, λ, ν, h, g and c are the carrier charge, visible wavelength, frequency of incident light, Plank constant, gain, and the speed of light, respectively.

The current gain was also calculated by using the following relation;

$$\text{Gain} = \frac{I_{ph}}{I_d} \tag{10}$$

The photocurrent gain is calculated to be 270.642 at 540 nm wavelength with illumination intensity of 1.535 mW/cm^2 and the bias voltage was 5 V. The values of photocurrent gain and sensitivity achieved in our photodetector are higher than the previously reported values.

Fig. 11 displays the equivalent rise in the photocurrent as a function of time at changed bias applied voltages with an interval of 20 s. The device was observed excellent stability and repeatability behaviour at various bias voltages. The results reveal a favourable various with time. The curves demonstrated rectangular shaped profiles, and the values of the photocurrent for every on/off cycle were stable and repeatable. The recovery and rise times for MSM photodetector were examined at different bias applied voltages are revealed in Fig. 11. The recovery time can be defined as the time for the current to decrease from 90% to 10% of its saturation value whereas rise time is the time for the current to increase from 10% to 90% of its saturation value. The rise and recovery time were also calculated from the current-time pulse graphs. The results for the device were noted to be obviously the short

time realized among the V_2O_5 detectors described in researches. Additionally, Table 1 recapitulates the responsivity, sensitivity values, response time and recovery time and of the MSM photodetector at 5 V bias applied voltages in the present work and the results achieved from the different types detectors in literature [1,26,45,46]. The fast photoresponse in the present work is associated to large photoactive surface areas and the high quality of the V_2O_5 NRs obtained on Si substrate. A fast response and recovery time shows that the vertical V_2O_5 NR based on Si substrate is convenient for good speed operation. Furthermore, the large photocurrent and responsivity values are assigned to more carriers collected under light in the V_2O_5 NR thin films. These results exhibited that the V_2O_5 NRs MSM photodetector could be used in useful applications.

4. Conclusions

High crystallinity quality V_2O_5 NRs were prepared on silicon substrate using spray pyrolysis technique. MSM photodetector was fabricated successfully on the obtained V_2O_5 NRs/Si and investigated under illumination conditions. The results indicated the good stability, large photocurrent, high sensitivity and excellent responsivity of MSM photodetector upon exposure illumination to 540 nm at 1.535 mW/cm^2 power intensity with 5 V bias voltages. Moreover, the MSM photodetector revealed fast recovery and response time. The experimental results exhibit that the excellent crystallinity quality MSM photodetector is a favourable candidate for optoelectronic applications.

Acknowledgements

We gratefully acknowledge the support of the Universiti Sains Malaysia under RU Top Down grant (1001/CINOR/870019).

References

[1] T. Zhai, H. Liu, H. Li, X. Fang, M. Liao, L. Li, H. Zhou, Y. Koide, Y. Bando, D. Golberg, Centimeter-long V_2O_5 nanowires: from synthesis to field-Emission, electrochemical, electrical transport, and photoconductive properties, Adv. Mater. 22 (2010) 2547–2552.
[2] B.H. Kim, A. Kim, S.-Y. Oh, S.-S. Bae, Y.J. Yun, H.Y. Yu, Energy gap modulation in V_2O_5 nanowires by gas adsorption, Appl. Phys. Lett. 93 (2008) 233101.
[3] R. Tamang, B. Varghese, E.S. Tok, S. Mhaisalkar, C.H. Sow, Sub-bandgap energy photoresponse of individual V_2O_5 nanowires, Nanosci. Nanotechnol. Lett. 4 (2012) 716–719.
[4] A.A. Akl, Effect of solution molarity on the characteristics of vanadium pentoxide thin film, Appl. Surf. Sci. 252 (2006) 8745–8750.
[5] M. Abyazisani, M.M. Bagheri-Mohagheghi, M.R. Benam, Study of structural and optical properties of nanostructured V_2O_5 thin films doped with fluorine, Mater. Sci. Semicond. Process. 31 (2015) 693–699.
[6] M. Benmoussa, A. Outzourhit, A. Bennouna, E. Ameziane, Electrochromism in sputtered V_2O_5 thin films: structural and optical studies, Thin Solid Films 405 (2002) 11–16.
[7] R.R. Kumar, B. Karunagaran, D. Mangalaraj, S.K. Narayandass, P. Manoravi, M. Joseph, V. Gopal, R. Madaria, J. Singh, Room temperature deposited vanadium oxide thin films for uncooled infrared detectors, Mater. Res. Bull. 38 (2003) 1235–1240.
[8] V. Modafferi, S. Trocino, A. Donato, G. Panzera, G. Neri, Electrospun V_2O_5 composite fibers: synthesis, characterization and ammonia sensing properties, Thin Solid Films 548 (2013) 689–694.
[9] V. Parvulescu, S. Boghosian, V. Parvulescu, S. Jung, P. Grange, Selective catalytic reduction of NO with NH 3 over mesoporous V_2O_5–TiO_2–SiO_2 catalysts, J. Catal. 217 (2003) 172–185.
[10] G. Rizzo, A. Arena, A. Bonavita, N. Donato, G. Neri, G. Saitta, Gasochromic response of nanocrystalline vanadium pentoxide films deposited from ethanol dispersions, Thin Solid Films 518 (2010) 7124–7127.
[11] G.D.J. Smit, S. Rogge, T.M. Klapwijk, Enhanced tunneling across nanometer-scale metal-semiconductor interfaces, arXiv preprint cond-mat. (2011) 110256.
[12] L. Vikas, K. Vanaja, P. Subha, M. Jayaraj, Fast UV sensing properties of n-ZnO nanorods/p-GaN heterojunction, Sens. Actuators A: Phys. 242 (2016) 116–122.
[13] M. Rajabi, R. Dariani, A.I. Zad, UV photodetection of laterally connected ZnO rods grown on porous silicon substrate, Sens. Actuators A: Phys. 180 (2012) 11–14.
[14] G.M. Ali, J.C. Moore, A.K. Kadhim, C. Thompson, Electrical and optical effects of Pd microplates embedded in ZnO thin film based MSM UV photodetectors: a comparative study, Sens. Actuators A: Phys. 209 (2014) 16–23.
[15] J. Xing, H. Wei, E.-J. Guo, F. Yang, Highly sensitive fast-response UV photodetectors based on epitaxial TiO_2 films, J. Phys. D: Appl. Phys. 44 (2011) 375104.
[16] J. Musschoot, D. Deduytsche, H. Poelman, J. Haemers, R. Van Meirhaeghe, S. Van den Berghe, C. Detavernier, Comparison of thermal and plasma-enhanced ALD/CVD of vanadium pentoxide, J. Electrochem. Soc. 156 (2009) P122–P126.
[17] C. Zou, X. Yan, J. Han, R. Chen, W. Gao, Microstructures and optical properties of β-V_2O_5 nanorods prepared by magnetron sputtering, J. Phys. D: Appl. Phys. 42 (2009) 145402.
[18] D.V. Raj, N. Ponpandian, D. Mangalaraj, C. Viswanathan, Effect of annealing and electrochemical properties of sol?gel dip coated nanocrystalline V_2O_5 thin films, Mater. Sci. Semicond. Process. 16 (2013) 256–262.
[19] S. Beke, S. Giorgio, L. Kőrösi, L. Nanai, W. Marine, Structural and optical properties of pulsed laser deposited V_2O_5 thin films, Thin Solid Films 516 (2008) 4659–4664.
[20] A. Subrahmanyam, Y.B.K. Reddy, C. Nagendra, Nano-vanadium oxide thin films in mixed phase for microbolometer applications, J. Phys. D: Appl. Phys. 41 (2008) 195108.
[21] J. Mu, J. Wang, J. Hao, P. Cao, S. Zhao, W. Zeng, B. Miao, S. Xu, Hydrothermal synthesis and electrochemical properties of V_2O_5 nanomaterials with different dimensions, Ceram. Int. 41 (2015) 12626–12632.

[22] L. Kong, I. Taniguchi, Correlation between porous structure and electrochemical properties of porous nanostructured vanadium pentoxide synthesized by novel spray pyrolysis, J. Power Sources 312 (2016) 36–44.
[23] N. Abd-Alghafour, N.M. Ahmed, Z. Hassan, S.M. Mohammad, M. Bououdina, M. Ali, Characterization of V_2O_5 nanorods grown by spray pyrolysis technique, J. Mater. Sci.: Mater. Electron. 27 (2016) 4613–4621.
[24] R. Suresh, Effect of post-growth annealing on the structural optical and electrical properties of V_2O_5 nanorods and its fabrication, characterization of V_2O_5/p-Si junction diode, Mater. Sci. Semicond. Process. 41 (2016) 497–507.
[25] D. Dubal, D. Dhawale, A. More, C. Lokhande, Synthesis and characterization of photosensitive TiO_2 nanorods by controlled precipitation route, J. Mater. Sci. 46 (2011) 2288–2293.
[26] R.-S. Chen, W.-C. Wang, C.-H. Chan, H.-P. Hsu, L.-C. Tien, Y.-J. Chen, Photoconductivities in monocrystalline layered V_2O_5 nanowires grown by physical vapor deposition, Nanoscale Res. Lett. 8 (2013) 1–8.
[27] Y.-q. Wang, Z.-c. Li, Z.-j. Zhang, Preparation of V_2O_5 thin film and its optical characteristics, Front. Mater. Sci. China 3 (2009) 44–47.
[29] S. Pavasupree, Y. Suzuki, A. Kitiyanan, S. Pivsa-Art, S. Yoshikawa, Synthesis and characterization of vanadium oxides nanorods, J. Solid State Chem. 178 (2005) 2152–2158.
[30] N. Wang, Y. Zhang, T. Hu, Y. Zhao, C. Meng, Facile hydrothermal synthesis of ultrahigh-aspect-ratio V_2O_5 nanowires for high-performance supercapacitors, Curr. Appl. Phys. 15 (2015) 493–498.
[31] A. Moholkar, S. Pawar, K.Y. Rajpure, S.N. Almari, P. Patil, C. Bhosale, Solvent-dependent growth of sprayed FTO thin films with mat-like morphology, Sol. Energy Mater. Sol. Cells 92 (2008) 1439–1444.
[32] A.M. Selman, Z. Hassan, Highly sensitive fast-response UV photodiode fabricated from rutile TiO_2 nanorod array on silicon substrate, Sens. Actuators A: Phys. 221 (2015) 15–21.
[33] M. Kang, E. Oh, I. Kim, S.W. Kim, J.-W. Ryu, Y.-G. Kim, Optical characteristics of amorphous V_2O_5 thin films colored by an excimer laser, Curr. Appl. Phys. 12 (2012) 489–493.
[34] L.-J. Meng, R.A. Silva, H.-N. Cui, V. Teixeira, M. Dos Santos, Z. Xu, Optical and structural properties of vanadium pentoxide films prepared by dc reactive magnetron sputtering, Thin Solid Films 515 (2006) 195–200.
[35] C. Diaz-Guerra, J. Piqueras, Thermal deposition growth and luminescence properties of single-crystalline V_2O_5 elongated nanostructures, Cryst. Growth Des. 8 (2008) 1031–1034.
[36] M.-C. Wu, C.-S. Lee, Field emission of vertically aligned V_2O_5 nanowires on an ITO surface prepared with gaseous transport, J. Solid State Chem. 182 (2009) 2285–2289.
[37] B. Yan, L. Liao, Y. You, X. Xu, Z. Zheng, Z. Shen, J. Ma, L. Tong, T. Yu, Single-crystalline V_2O_5 ultralong nanoribbon waveguides, Adv. Mater. 21 (2009) 2436–2440.
[38] B. Bera, A. Esther, A. Dey, A. Mukhopadhyay, Structural, optical and electrical properties of V_2O_5 xerogel thin films, Indian J. Phys. 90 (2016) 687–692.
[39] S. Inamdar, V. Ganbavle, K. Rajpure, ZnO based visible–blind UV photodetector by spray pyrolysis, Superlattices Microstruct. 76 (2014) 253–263.
[40] F.K. Butt, C. Cao, F. Idrees, M. Tahir, R. Hussain, A.Z. Alshemary, Fabrication of V_2O_5 super long nanobelts: optical, in situ electrical and field emission properties, New J. Chem. 39 (2015) 5197–5202.
[41] M.S. Raman, J. Chandrasekaran, R. Priya, M. Chavali, R. Suresh, Effect of post-growth annealing on the structural optical and electrical properties of V_2O_5 nanorods and its fabrication, characterization of V_2O_5/p-Si junction diode, Mater. Sci. Semicond. Process. 41 (2016) 497–507.
[42] M. Benmoussa, E. Ibnouelghazi, A. Bennouna, E. Ameziane, Structural, electrical and optical properties of sputtered vanadium pentoxide thin films, Thin Solid Films 265 (1995) 22–28.
[43] H. Huang, Y. Xie, Z. Zhang, F. Zhang, Q. Xu, Z. Wu, Growth and fabrication of sputtered TiO_2 based ultraviolet detectors, Appl. Surf. Sci. 293 (2014) 248–254.
[44] W. Zhang, J. Zhao, Z. Liu, Z. Liu, Z. Fu, Influence of growth temperature of TiO_2 buffer on structure and PL properties of ZnO films, Appl. Surf. Sci. 256 (2010) 4423–4425.
[45] M.S. Pawar, P.K. Bankar, M.A. More, D.J. Late, Ultra-thin V_2O_5 nanosheet based humidity sensor, photodetector and its enhanced field emission properties, RSC Adv. 5 (2015) 88796–88804.
[46] J. Lu, M. Hu, Y. Tian, C. Guo, C. Wang, S. Guo, Q. Liu, Fast visible light photoelectric switch based on ultralong single crystalline V_2O_5 nanobelt, Opt. Express 20 (2012) 6974–6979.
[47] N. Hassan, M. Hashim, Flake-like ZnO nanostructures density for improved absorption using electrochemical deposition in UV detection, J. Alloys Compd. 577 (2013) 491–497.

Biographies

Nabeel Mohammed Abd-Alghafour received the B.Sc degree in physics from Al-Anbar University-Iraq-1995 and Master's Degree in physics from Al-Anbar University-Iraq-in 2010. He worked with Iraqi Ministry of Education as a physics teacher in Anbar from 1998. He has been a Ph.D student at University Sains Malaysia-School of Physics-Nano-Optoelectronics Research and Technology Laboratory Since 2014. Along with his Ph.D study, he's currently a Research Associate at University Sains Malaysia USM) and has published to 6 papers in nanotechnology and nano-optoelectronic devices.

Naser Mahmoud received the B.Sc degree in physics from Al-Mustanseriah University Iraq in 1984, Master's Degree in Laser Technology from University of technology, Iraq in 1988, and Ph.D degree in Solid State Physics and Nanotechnology from University Sains Malaysia, Malaysia in 2006. He was a Research Associate at University Sains Malaysia from 2003 to 2006. At present, he is an assistant Professor of school of physics USM. His work on Laser and optoelectronic materials and devices has led to over75 published papers and six books in Laser and nanotechnology.

Zainuriah Hassan received the B.Sc (Magna Cum Laude) degree and the Master's degree in Physics from Western Michigan University, USA in 1983 and 1985, respectively, and Ph.D degree in Experimental Condensed Matter Physics from Ohio University, USA in 1998. She was a Research Associate at Ohio University from 1997 to 1998, and a Visiting Research Scholar under the Fulbright Program at Department of Electrical and Computer Engineering, University of Minnesota, USA in 2004/2005. At present, she is the Director of the Center for Research Initiatives in Natural Sciences at Universiti Sains Malaysia, and formerly the Dean, Deputy Dean (Academic and Student Development) and Chair of the Engineering Physics Program at School of Physics, Universiti Sains Malaysia. She was promoted to Professor in 2009 and is attached to the Condensed Matter, Applied and Engineering Physics group. She has received several national and international awards and scholarships, and served as reviewers, jury, and members of various committees. Her focus of research is on all aspects related to materials growth, characterization, and fabrication of optoelectronic and electronic devices such as sensors based on III-nitrides (GaN, InN, AlN, and related nitride alloys) and also other wide band gap semiconductors such as ZnO, CdS, TiO_2, CdO and other metallic oxides. She has published more than 500 papers in international and national journals and proceedings. She is currently the Editor of Journal of Physical Science and a member of the Materials Research Society, Optical Society of America, IEEE, Fulbright Association, Malaysian Solid State Science and Technology Society, Malaysian Institute of Physics, and National Council of Professor.